Innovative and stable TiO2 supported catalytic surfaces removing aldehydes under UV-light irradiation

W. Elfalleh, A. A. Assadi, A. Bouzaza, D. Wolbert, J. Kiwi, S. Rtimi

Innovative and stable TiO_2 supported catalytic surfaces removing aldehydes under UV-light irradiation.

W. Elfallah [1], A. A. Assadi [2]*, A. Bouzaza [2], D. Wolbert [2], J. Kiwi [3], S. Rtimi [4]**

[1] *Unité de Recherche Catalyse et Matériaux pour l'Environnement et les Procédés URCMEP (UR11ES85), Université de Gabès, Campus Universitaire Cité Erriadh, Gabès 6072, Tunisia.*

[2] Laboratoire *Sciences Chimiques de Rennes-équipe Chimie et Ingénierie des Procédés, UMR 6226 CNRS, ENSCR-11, allée de Beaulieu, CS 508307-35708 Rennes, France.*

[3] Ecole *Polytechnique Fédérale de Lausanne, EPFL-SB-ISIC-GPAO, Station 6, CH-1015 Lausanne, Switzerland.*

[4] Ecole *Polytechnique Fédérale de Lausanne, EPFL-STI-IMX-LTP, Station 12, CH-1015 Lausanne, Switzerland.*

* Corresponding authors : aymen.assadi@ensc-rennes.fr (A. Assadi).
sami.rtimi@epfl.ch (S. Rtimi)

Abstract

The present study reports the photocatalytic degradation of aldehydes using TiO_2 impregnated polyester (PES) and glass fiber (GFT)-TiO_2 addressing the photocatalytic degradation aldehydes (air-solid interface). The PES-TiO_2 optical absorption was determined by diffuse reflectance spectroscopy (DRS). By X-ray diffraction (XRD), the formation of TiO_2 anatase on the PES surface was detected. The photocatalytic oxidation (PCO) of butyraldehyde and isovaleraldehyde was carried out in a batch photo-reactor equipped with a UV-mercury Philips 9W lamp and mediated by glass fiber GFT-TiO_2 and PES-TiO_2 surfaces. The removal of these two aldehydes was found to be a function of pollutant concentrations. The stable catalytic reuse of both catalysts reported. A Langmuir Hinshelwood (L-H) model describes the degradation kinetics on PES-TiO_2 and on GFT-TiO_2. The aldehyde degradation by-products were analyzed by gas chromatography mass spectrometry (GC-MS). Three organics intermediates identified during the aldehyde degradation were: acetones, alcohols and fatty acids.

Keywords:

TiO_2-PES; batch photo-reactor; kinetics; intermediate by-products, GC-MS, L-H isotherms, degradation kinetics

Introduction:

VOCs have been found to be hazardous to the human health and introduce collateral environmental damage. VOCs are discharged into the atmosphere by households and industry, and found in the exhaust gases from animal quartering, and residential cleaning agents. Damaging health effects have been reported on the eyes, nose and throat. They also lead to headaches, loss of coordination and nausea, damages to the liver, kidney and the central nervous system [1]. Moreover, they can induce cancer in animals; and can cause cancer in humans [2]. The technologies developed until now to remove VOCs have not been entirely successful and do not meet the regulatory levels becoming more demanding during the last decade. Recently studies report the aldehyde removal by adsorption [3], biological treatment [4] and advanced oxidation processes (AOP's).

Photocatalytic TiO_2 materials have been widely used during the last four decades due to their low cost, photo-activity and stability [5]. TiO_2 is widely used in catalytic processes occurring at the air-solid interface at room temperature and atmospheric pressure [6–8]. TiO_2 (titania) stands out as one of the most active photocatalyst [9] under UV-radiation. The electrons in the valence band of TiO_2 under light move to the conduction band generating electron (e^-)-hole (h^+) pairs. These electrons in contact with air are able to reduce the O_2 forming superoxide ions. Moreover, the holes oxidize water adsorbed on the TiO_2-surface generating hydroxyl radical (HO°) [10-11]. The later radical species oxidize organic compounds to produce CO_2 [12,13-15]. TiO_2 has been also used in chemical synthesis [16,17] and energy conversion [18].

Many research groups studied the photocatalytic oxidation for indoor and outdoor cleaning under UV and/or solar light. The reaction rate of a photocatalytic reaction depends on the catalyst, the applied light intensity, the concentration of reactants (in our case gaseous effluents), the flow rate and the type of reactor used (batch or continuous) [9,12].

This paper presents the optimization for the TiO_2 impregnation on two supports: polyester (from now PES) and Glass Fiber Tissue (from now GFT). It reports some properties of these surfaces [19] along the Langmuir Hinshelwood (L-H) isotherm followed during the photocatalytic degradation of the two aldehydes. The first

evidence for the degradation kinetics for gas-phase PCO of aldehydes is presented on PES-TiO_2 and GFT-TiO_2. Butyraldehyde and isovaleraldehyde were chosen as probes due to their abundant presence in exhaust gases from animal process/quartering [20].

2. Experimental Section

2.1. Chemical reagents

Chemicals were Sigma–Aldrich (USA). The isovaleraldehyde (≥ 98%) and butyraldehyde (≥99%) were p.a. reagents and used as received. Both aldehydes belong to the priority group of VOCs pollutants: aromatics (one, two or three rings) alkanes, ketones, alcohol, and chloro-carbons by the French Environment and Energy Management Agency (ADEME).

2.2. Apparatus and Analysis:

The batch reactor used was approximately 400 mm high and was able to contain a volume of 1.5 L. The catalytic samples used presented a surface of 330 cm^2 and were attached to the inner wall of the cylindrical reactor. The fluorescent UV-lamp in the photo-reactor was Philips PL-S 9W/10/4P. The outside wall of the reactor was covered with Al-foil during the irradiation experiments to prevent the lamp UV-emission to reach the outside of the reactor. A magnetic stirrer and a magnetic barrel allowed the homogenization of the gas phase.

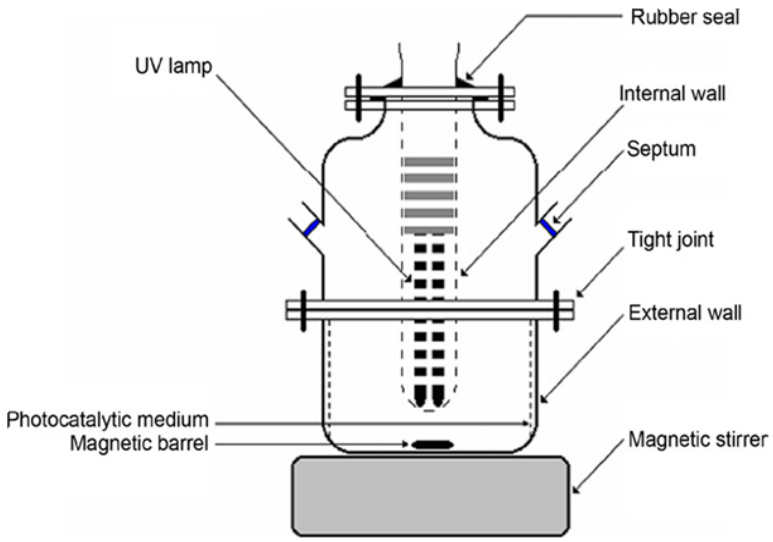

Figure 1. Schematic of the batch photo-reactor with the central co-axial mercury 9W mercury UV-light source

During the course of this study a aldehyde samples were injected into the reactor. A magnetic stirrer and some glass spheres were used to homogenize of the inlet gas phase. When the equilibrium was reached, the UV lamp was turned on. Samples were taken regularly from the reactor for analysis.

The main reaction intermediates present in gas phase were analyzed to suggest at later stages during this study a reaction mechanism. Carbotrap compositions were used to concentrate the pollutiants: Carbopack Y, is used for the selective retention of the C_{12} to C_{20} compounds. By way of Carbopack B C_5 to C_{12}, compounds were trapped while the lighter compounds C_2 to C_5 were adsorbed with Carboxen 1003. The initially concentrated aldehydes on different Carbotrap (Supelco) were then pumped by a a Gillian LFS-113 pump under a flow rate of 50 mL/min. Subsequently, a Turbomatrix Perkin Elmer unit was used to thermally desorb these concentrated compounds. Then the gases were analyzed through a transfer line to the GC/MS Perkin Elmer Clarus 500 equipped with a Quadrupole mass spectrometer detector. The GC/MS column consisted of a capillary column FFAP-CB Chrompact 25 m long, 0.15 mm in diameter and a stationary phase's thickness of 0.25 µm. The temperature in the oven, the injection chamber and the detector were 100, 120 and 200 °C respectively.

2.3. Catalyst

2.3.1. Glass Fiber Tissue (GFT)

The glass-fiber(GFT) was provided by Ahlstrom Research/Services [12]. This material contained colloidal silica, a variable percentage of titanium dioxide, manganese dioxide nanoparticles and inorganic fibers as shown in Figure 2a. TiO_2 was deposited on the inorganic fibers by impregnation using an industrial-size press as shown in Figure 2b. A mixture of 50-wt% colloidal silica and different wt% of TiO_2 nanoparticles (PC500 Millennium) and manganese dioxide is suspended in pure water. In order to ensure the deposition of 13 g/m^2 of dry TiO_2 on the GFT support. The suspension was composed of 40% of dry powder and 60% of pure water. The PC500 TiO_2 nanoparticles consisted of anatase 5-10 nm in diameter with and TiO_2 SSA nanoparticles of 300 m^2/g as shown in Figure 2a.

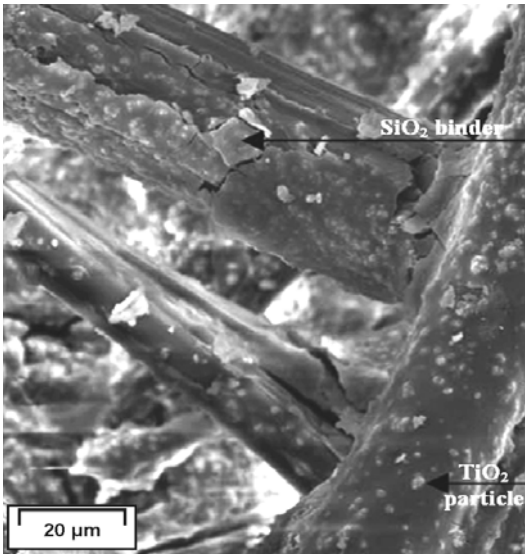

Figure 2a. Scanning electron micrographs **(**SEM) of the glass fibers (GFT).

An industrial type press was employed to impregnate fibers with the TiO_2 suspension, followed by the drying cstep arried out by Ahlstrom Research and Services.

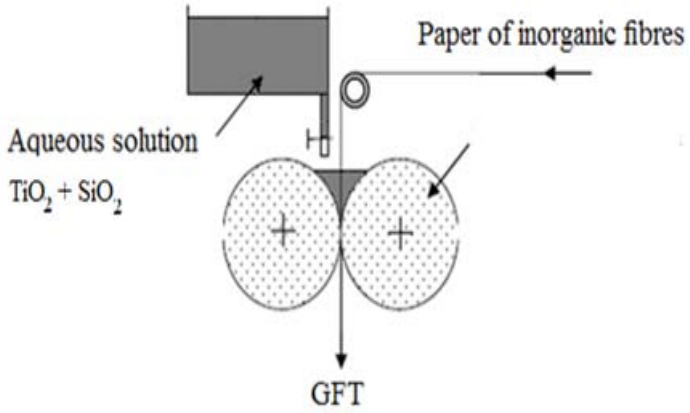

Figure 2b. Diagram of the impregnation technique for GFT synthesis "size press"

2.3.2. TiO_2 impregnated PES: TiO_2 loading, spectral absorption and isoelectric point.

PES-TiO_2 samples were prepared hydrothermal (HT) preparation treatment method. During the HT-preparation, the TiO_2 colloidal suspension was prepared dissolving titanium tetra-isopropoxide (TTIP, Sigma Aldrich) in isopropanol in a 1:3 volume ratio. Then, the solution was transferred into a beaker with 50 ml of 0.1M HNO_3. This way of preparation lead to a substantial TiO_2 aggregation. To study the effect of these aggregations on the photocatalytic activity, some samples were ultra-sonicated for 10 min prior to the PES impregnation; these samples will be called US-TiO_2-PES along the manuscript. The polyester samples 10x10 cm was immersed into the acid TiO_2 precursor suspension and heated under stirring in a reflux condenser

for 2 hours at 80°C. The PES fabric was removed from the suspension, rinsed with demineralized water and treated in ultrasound bath for 2 min to remove the unbounded TiO_2 particles. The last operation was repeated three times and the TiO_2-polyester fabric dried for 2 hours in air at 70°C.

The low surface energy of polyester led to poor TiO_2 nanoparticles adhesion. In order to fix a higher amount of TiO_2 on PES, the PES was pretreated by UVC-light to induce a higher density of functional polar groups able to bind TiO_2 nanoparticles [21]. UVC pretreatment enhances the polarity, roughness and hydrophilicity of polyester improving its bondability and interfacial adhesion. The UVC pre-treatment induced negatively charged functional groups, e.g., carboxylic, percarboxylic, epoxide and peroxide groups due to the atomic and excited-O*. The polyester negative sites bind the slightly positive deposited $Ti^{4+}/(TiO_2)$ by electrostatic attraction involving chelation/complexation [23]. The TiO_2 was deposited immediately after the UVC-pretreatment due to the short lifetimes of the polar radical species.

To determine the TiO_2 isoelectric point (IEP), a Colloidal Dynamics Acousto Sizer II (Sydney, Australia) instrument was used. The zeta potential is calculated from the widely used Smoluchowski equation [23, 24] for thin double layers (ka >20). The electro-acoustic determines the dynamic mobility, of the suspensions in 150 ml KNO_3 (0.01M). The pH adjusted with HNO_3 to around 3 and then titrated up to pH 10 or 11 by addition of KOH (0.01 M) 25°C. The colloid was dispersed under vigorous agitation and ultrasonic treatment for 5 minutes (150 watts, 20 kHz).

The Ti-content of the TiO_2-PES samples was determined in an Orbis PC Micro EDXRF analyzer equipped with a Rh micro-focus X-ray tube (50 kV and 1 mA) and X-ray multiple optic turret with 30 µm poly-capillary X-Ray optics/collimator.

Diffuse reflectance spectroscopy (DRS) was carried out in a Varian Analytical Instruments Cary 5 UV-VIS-IR spectrophotometer (controlled by the Cary Win UV software) within the wavelength range of 300-800 nm and a resolution of one nm. The spectral absorption of the samples was plotted in the Kubelka-Munk (KM) units vs. wavelength.

2.4. Pollutants degradation conditions

Degradation of isovaleraldehyde and butyraldehyde in the photocatalytic reactor was evaluated for several influent pollutant concentrations (Table 1).

Table 1. Experimental Conditions used during the degradation of aldehydes in the batch photo-reactor.

Parameter	Value & domain
Gas Temperature	Ambient (293 K)
Gas Pressure	Atmospheric pressure (1 atm)
Volume of reactor	1 L
Isovaleraldehyde Inlet Concentration [Isoval]	1 to 22 g/m^3
Butyraldehyde Inlet Concentration [Buty]	1 to 20 g/m^3
Relative humidity	40-50 %
Intensity of UV lamp	30 W/m^2

3. Results and discussion

3.1. TiO_2 loading, IEP and spectral absorption

By X-ray fluorescence (XRF), HT PES-TiO_2 samples were found to have a 0.61 wt%TiO_2 / wt PES loading and the US PES-TiO_2 samples presented a TiO_2 loading of 0.39 wt%TiO_2 / wt PES. The quantity of TiO_2 was not very high as to affect the PES flexibility and/or other mechanical properties.

Figure 3 shows the spectral absorption of TiO_2-impregnated polyester prepared by both preparation methods HT or US.

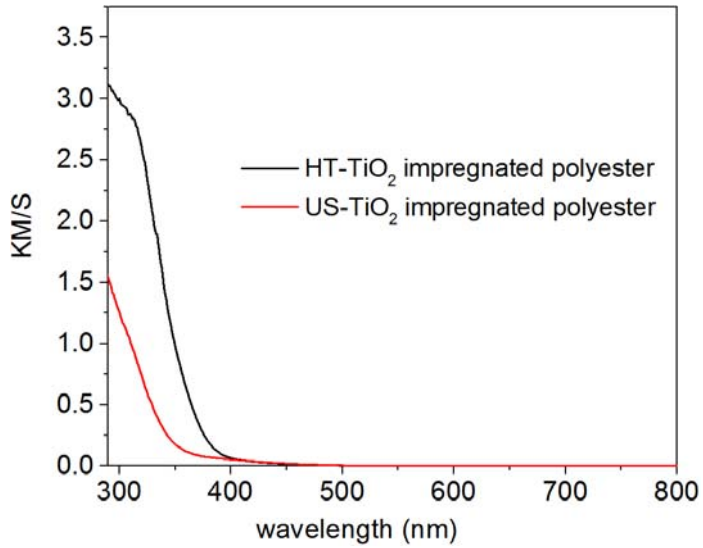

Figure 3. Diffuse reflection spectroscopy **(**DRS) absorption of PES-TiO_2.

The diffuse reflectance spectra (DRS) in Figure 3 show a higher optical absorption for the samples prepared by the HT-method compared to the samples prepared by the US-method. The higher TiO_2 loading on the HT-samples explains these DRS results as determined by (XFR) and can be explained by the different

aggregation of the TiO_2 clusters on the polyester surface. This leads to light reflectance in all directions increasing the signal registered in the optical integration sphere.

The rough UV-Vis reflectance data cannot be used directly when accounting for the absorption coefficient of the TiO_2-impregnated polyester due to the large scattering contribution. Normally, a weak dependence is assumed for the scattering coefficient S on the light diffusion.

In agreement with the Derjaguin-Landau-Verwey-Overbeek (DLVO) theory of colloidal stability, nanoparticle aggregation sets in at pH close to the TiO_2 IEP 6-7 used during the preparation of the TiO_2 colloidal suspensions due to the attractive Van der Waals forces. The TiO_2 single particles present sizes between 40-60 nm. The hydrodynamic diameter of the aggregates was found to be 170-240 nm and is approximately equivalent to 3-6 primary TiO_2 particles [19], aggregates involve a higher mass of TiO_2 but a lower surface *per* particle active intervening in the photocatalytic process.

3.2. Pollutant degradation

To separate the effects of photocatalysis and adsorption, the VOC with a concentration of several g/m^3 were mixed with air and stirred for 30 min in the dark to reach adsorption-desorption equilibrium at time zero. Subsequently, the mixture was irradiated under UV-light for 180 min to test the photo-activity of PES-TiO_2. After the experimental conditions became stable, the PCO reaction was initiated and the VOC injected. Under steady-state conditions samples were taken to evaluate the degradation rate and the generation of by-products

Figure 4a and b show the variation of isovaleraldehyde) and butyraldehyde concentrations versus time at different inlet concentrations. The degradation rate first increased with the inlet concentration, due to the availability of the photocatalytic sites at a low concentration range [9, 11].

The concentrations of both aldehydes shown in Figures 4a/4b decreased with increasing irradiation time, going from 10 to 3 g/m^3 and from 9 to 0.8 g/m^3 within 15 min irradiation, at inlet concentration values of 10 and 9 g/m^3 respectively. These rates were similar to the values reported for some VOCs [11-14]. We suggest that the degradation mechanism of the aldehydes on supported-TiO_2 involve TiO_2 electrons in the conduction band (cb) reacting with adsorbed O_2 on the TiO_2 yielding HO_2°

radical-anions and other highly oxidative protonated radicals leading to the oxidation of the aldehydes [10, 21-23].

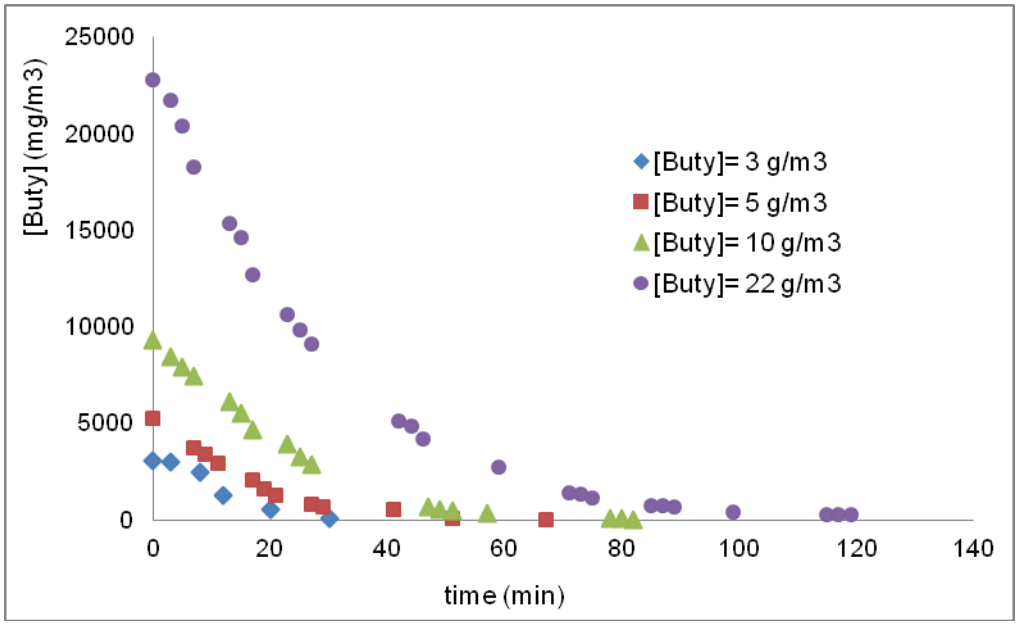

Figure 4a. Butyraldehyde degradation on PES-TiO_2 as a function of the initial aldehyde concentration) under a Philips UV 9W mercury lamp irradiation (I=30W/m^2).

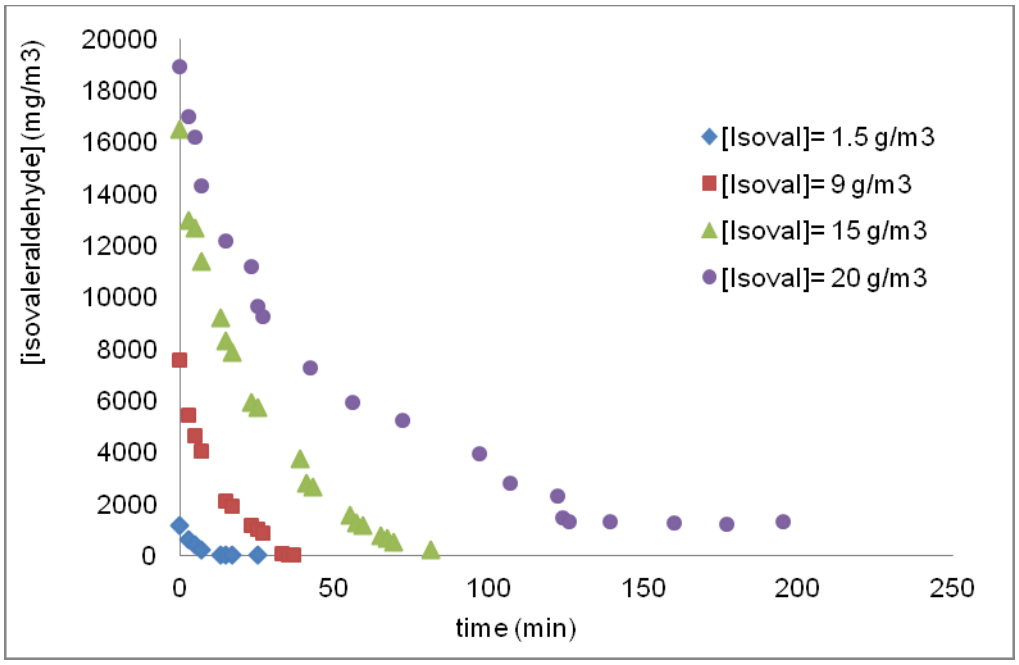

Figure 4b. Isovaleraldehyde degradation on PES-TiO_2 as a function of the initial aldehyde concentration under a Philips UV 9W mercury lamp (I=30W/m^2) irradaition.

3.3. Comparison with other photocatalyst (GFT)

The PES-TiO_2 and the (GFT)-TiO_2 samples presented a similar TiO_2 loading as determined by XRF of 0.61 wt%/wt-PES and 0.57 wt%/wt-GFT. PES and GFT did not led to aldehyde degradation in the dark or under light irradiation. Butyraldehyde, removal on GFT was about twice faster compared to PES, it reaches 90% removal in 30 minutes on GFT-TiO_2 as seen in Figure 5a. On PES-TiO_2 about 90% of butyraldehyde was removed within 60 min. The TiO_2 accessibility to lower depths in the GFT glass-wool containing TiO_2 dispersed nanoparticles offer a higher number of active sites *per* nanoparticle in the glass wool compared to the PES support. [14].

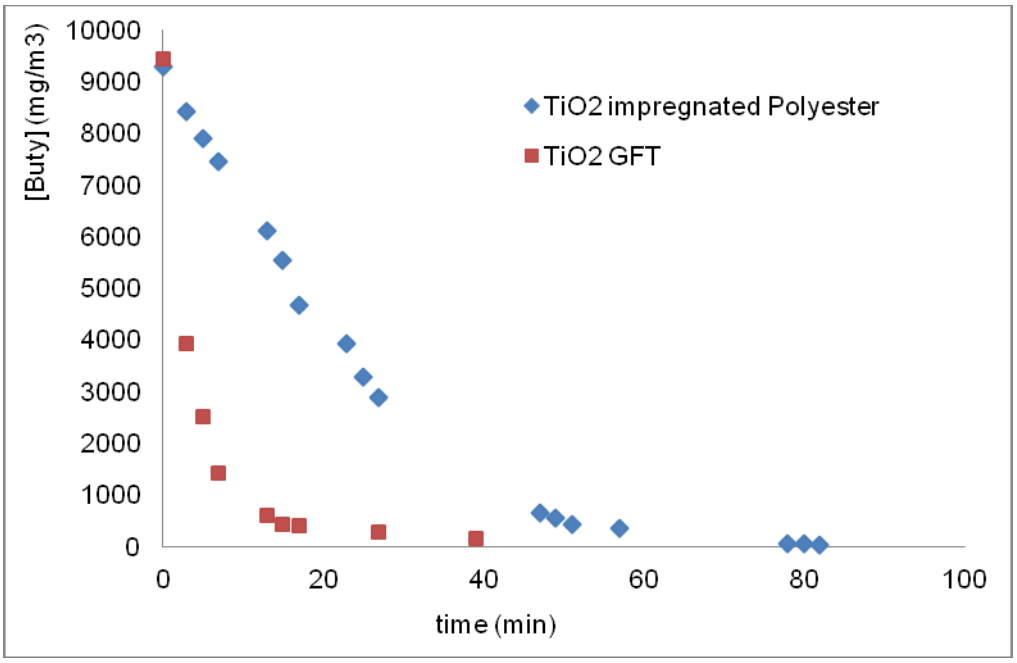

Figure 5a. Butyraldehyde photodegradation kinetics on GFT-TiO_2 and PES-TiO_2 samples under a Philips UV 9 W mercury lamp irradiation (I=30W/m^2).

To understand the kinetic and the adsorption process of butyraldehyde degradation on the two catalysts under investigation, the Langmuir-Hinshelwood (L-H) model was used according to the equation:

$$r_0 = -\frac{d[VOC]}{dt} = k_c \frac{K[VOC]_0}{1 + K[VOC]_0}$$

Where r_0 (mmol/g_{cat}xm^3xs) is the initial photocatalytic degradation rate, [VOC] is the initial butyraldehyde concentration (mmol/m^3), K is the adsorption constant (m^3/mmol) and kc is the kinetic constant (mmol.m^{-3}xsxgTiO_2) at maximum coverage for the experimental conditions used could be expressed as:

$$k_c = k_0 \times I^{\delta}$$

where I is the light intensity (W/m^2), k_0 is a rate constant independent of the light intensity and δ is the order of I ($0 < \delta < 1$).

The linearized L-H equation reads:

$$\frac{1}{r_0} = \frac{1}{k_c K} \times \frac{1}{[VOC]_0} + \frac{1}{k_c}$$

The plot of $1/r_0$ versus $1/[VOC]_0$ allows to determine k_c and K values by the plot presented in Figure 5b.

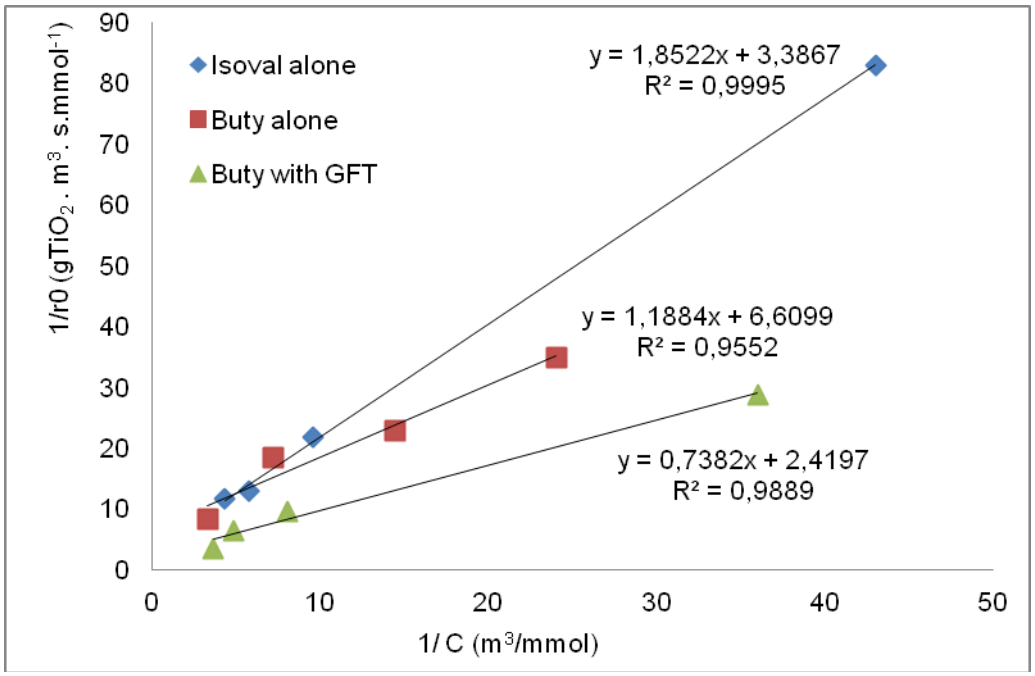

Figure 5b. Linear regression using L-H model for the butyraldehyde degradation and isovaleraldehyde alone and in the presence of GFT-TiO_2

According to the values reported in Figure 5b, the values of the L-H constants (k_c and K) are shown in the Table 2.

Table 2. L-H constants (k_c and K) at different catalysts tested

Catalyst tested	Target pollutant	k_c: Kinetic constant of L-H ($mmol.m^{-3}.s.g_{TiO2}$)	K: Adsorption Constant of L-H ($m^3.mmol^{-1}$)
PES-TiO_2	Isovaleraldehyde	0.2953	1.8285
	Butyraldehyde	0.1513	5.5545
GFT-TiO_2	Butyraldehyde	0.4134	3.2769

Table 2 shows that GFT-TiO_2 leads to a faster butyraldehyde degradation compared with the PES-TiO_2. Anatase crystals are formed at around 300°C and rutile at around 600°C when heating TiO_2 colloids in the absence of a structure-forming surface like polyester [19,28]. These temperatures are significantly higher compared to temperatures of around 80°C used in the preparation of TiO_2-polyester surfaces (see section 2.3.2). This can lead to different crystallographic structures influencing the photocatalytic activity as recently reported [10,19]. These support materials present: a) a different catalytic site accessibility for the aldehyde and b) a distinct light exposure of the TiO_2 sites to the incoming UV-light [14].

3.4. By-products Identification

The by-products detected during the photocatalytic degradation of butyraldehyde on PES-TiO_2 were determined by GC-MS. The degradation by-products detected were: methanol (2) acetone (3), ethyl acetate (4), acetic acid (5) and propionic acid (6). Butyraldehyde (1) was also present after 30 minutes. These results are similar to those reported by Assadi et al. [25, 26], reporting acetic, propionic, and butyric acids. Assadi el al., used GFT-TiO_2 for the isovaleraldehyde photodegradation and detected propionic acid, acetone, acetic acid and CO_2 as the degradation products.

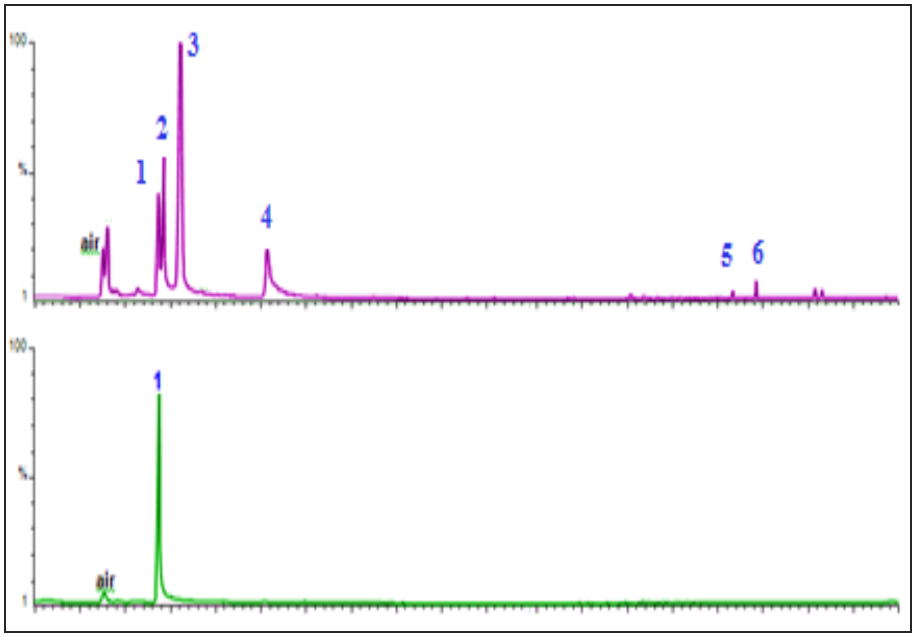

Figure 6. By-products observed during butyraldehyde degradation by GC–MS on PES-TiO_2

4. Catalyst recyclability

The reusability of the used catalyst is an important factor to investigate since it is a measure for its practical application potential degrading pollutants in the gas phase [27-28]. The repetitive use of the GFT-TiO_2 photocatalyst up to the 5^{th} cycle leading to butyraldehyde degradation is shown below in Figure 7. No loss of activity was detected by the photocatalyst during its repetitive recycling as shown in Figure 7. The catalyst was thoroughly washed after each photodegradation cycle and reused. The results reported in Figure 7 show the potential of the GFT-TiO_2 samples for application in air treatment.

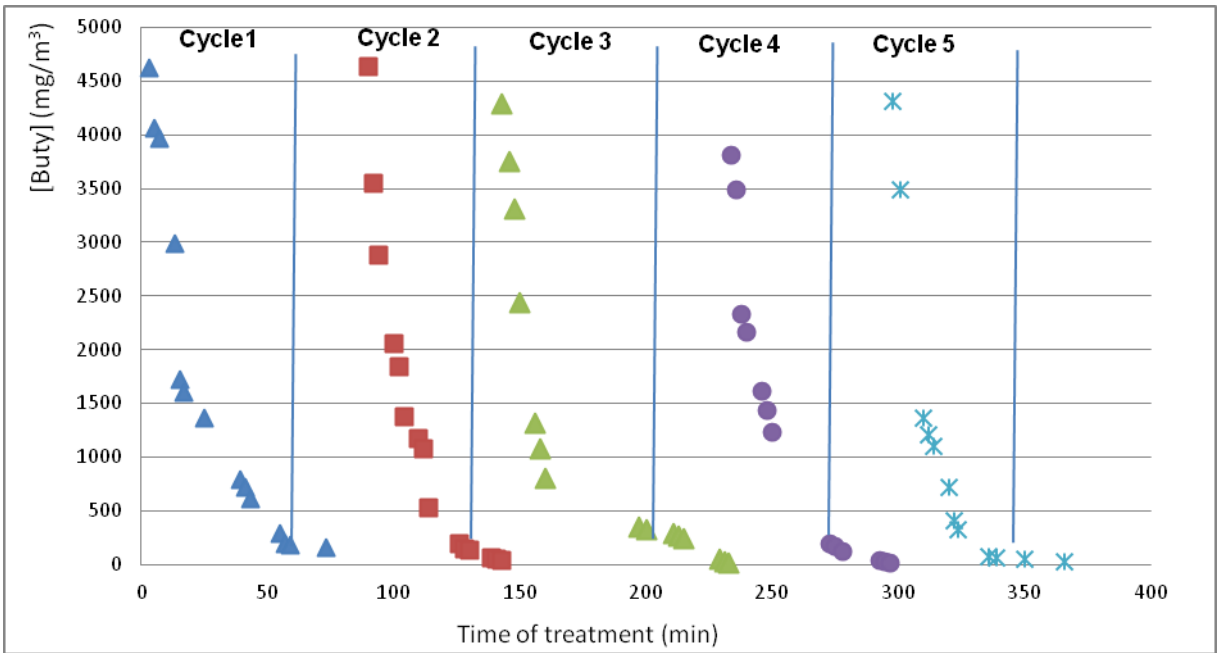

Figure 7. Repetitive degradation of butyraldehyde on a GFT-TiO_2 sample under 9W Philips mercury light. Further experimental conditions: I=30W/m^2, butyraldehyde concentration = 5 g/m^3.

5. Conclusion

Butyraldehyde and isovaleraldehyde degradation mediated by PES-TiO_2 and GFT-TiO_2 under mercury UV-light have been reported in this study. The by-products during the photocatalytic degradation of butyraldehyde on PES-TiO_2 were identified by GC-MS. The GFT-TiO_2 presented a larger photo-activity compared to PES-TiO_2 and this comparison was quantified by the k_c values found during in the L-H treatment of the experimental data. A stable degradation performance of the

aldehydes by the GFT-TiO_2 samples was observed during repetitive recycling under UV-light irradiation. This catalyst presents an application potential for application in air treatment.

References:

[1] Peter J. O'Brien, Arno G. Siraki & Nandita Shangari, Aldehyde Sources, Metabolism, Molecular Toxicity Mechanisms, and Possible Effects on Human Health, Critical Reviews in Toxicology 35 (2005) 609-662.

[2] d'Henry A. Heck, Mercedes Casanova & Thomas B. Starr, Formaldehyde Toxicity—New Understanding, Critical Reviews in Toxicology 20 (2008) 397-426.

[3] G. Gabrielson, Adsorption of aldehydes and ketones on anion exchangers in cyanide form, J. Chemical Technology and Biotechnology, 7 (1957) 533-535.

[4] P.M. Huck, W.B. Anderson, S.M. Rowley, S.A. Daignault, Formation and removal of selected aldehydes in a biological drinking-water treatment process, Aqua 39 (1990) 321-333.

[5] A.A. Assadi, A. Bouzaza, C. Vallet, D. Wolbert, Use of DBD plasma, photocatalysis, and combined DBD plasma/photocatalysis in a continuous annular reactor for isovaleraldehyde elimination–synergetic effect and byproducts identification, Chem. Eng. J. 254 (2014) 124-132.

[6] Y. Boyjoo, H.i Sun, J. Liu, V. K. Pareek, S. Wang, A review on photocatalysis for air treatment: From catalyst development to reactor design, Chemical Engineering Journal 310 (2017) 537-559.

[7] M. Robotti, S. Dosta, C. Fernández-Rodríguez, M.J. Hernández-Rodríguez, I.G. Cano, E. Pulido Melián, J.M. Guilemany, Photocatalytic abatement of NOx by C-TiO_2/polymer composite coatings obtained by low pressure cold gas spraying, Applied Surface Science, 362, 2016, 274-280.

[8] M. S. Curcio, M. P. Oliveira, W. R. Waldman, B. Sánchez, M. C. Canela, TiO_2 sol-gel for formaldehyde photodegradation using polymeric support: photocatalysis efficiency versus material stability, Environ Sci Pollut Res (2015) 22:800-809

[9] L. Zhong, F. Haghighat, C-S. Lee, N. Lakdawala, Performance of Ultraviolet Photocatalytic Oxidation for Indoor Air Applications: Systematic Experimental Evaluation, Journal of Hazardous Materials 261 (2013) 130-138.

[10] S. Rtimi, R. Sanjines, M. Andrzejczuk, C. Pulgarin, A. Kulik, J. Kiwi, Innovative transparent non-scattering TiO_2 bactericide thin films inducing increased *E. coli* cell wall fluidity, Surface and Coatings Technology 254 (2014) 333-343.

[11] T. Ochiai, A. Fujishima, Photoelectrochemical properties of TiO_2 photocatalyst and its app,ications for environmental purification, J. Photochem. Photobiol. C: Photochem. Rev. 13 (2012) 247-262.

[12] L. Zhong, Haghighat, F. Photocatalytic air cleaners and materials technologies abilities and limitations, Building and Environment, 91(2015) 191-203.

[13] A. A. Assadi, A. Bouzaza, D. Wolbert, P. Petit, Isovaleraldehyde elimination by UV/TiO_2 photocatalysis: comparative study of the process at different reactors configurations and scales, Environmental Science and Pollution Research, 21 (2014) 11178-11188.

[14] GL. Puma, V. Puddu, HK. Tsang, A. Gora, B. Toepfer, Photocatalytic oxidation of multicomponent mixtures of estrogens (estrone (E1), 17β-estradiol (E2), 17α-ethynylestradiol (EE2) and estriol (E3)) under UVA and UVC radiation: photon absorption, quantum yields and rate constants independent of photon absorption. Applied Catalysis B Environ 99 (2010) 388-397.

[15] AY. Shan, TIM. Ghazi,SA. Rashid, Immobilisation of titanium dioxide onto supporting materials in heterogeneous photocatalysis: a review. Applied Catalysis A: General 389 (2010) 1-8.

[16] R C. Suciu, E. Indrea, TD. Silipas, S. Dreve, MC. Rosu, V. Popescu, G. Popescu, HI. Nascu, TiO_2 thin films prepared by sol-gel method. J. Phys. Conf. Ser. 182 (2009) 012080.

[17] TK. Tseng, YS. Lin, YJ. Chen, H. Chu, A review of photocatalysts prepared by sol-gel method for VOCs removal. Int. J. Mol. Sci. 11 (2010) 2336-2361.

[18] T. Ochiai, T. Hoshi, H. Slimen, K. Nakata, T. Murakami, H. Tatejima, Y. Koide, A. Houas, T. Horie, Y. Moritobe, A. Fujishima, Fabrication of a TiO_2 nanoparticles impregnated titanium mesh filter and its application for environmental purification, Catal. Sci. Technol, 1 (2011) 1324-1327.

[19] J. Nesic, S. Rtimi, D. Laub, G. Roglic, C. Pulgarin, J. Kiwi, New evidence for TiO_2 uniform surfaces leading to complete bacterial reduction in the dark: Critical issues, Colloids and Surfaces B: Biointerfaces 123 (2014) 593-599.

[20] International Programme on Chemical Safety (IPCS), OECD screening information databases 3-methyl butanal, UNEP Canadian Centre for Occupational Health and Safety (CCOHS), 2004.

[21] S. Rtimi, C. Pulgarin, R. Sanjinesb, J. Kiwia, Novel FeOx–polyethylene transparent films: synthesis and mechanism of surface regeneration, RSC Advance 5 (2015) 80203-80211.

[22] H. Ourrad, F. Thevenet, V. Gaudion, V. Riffault, Limonene photocatalytic oxidation at ppb levels: Assessment of gas phase reaction intermediates and secondary organic aerosol heterogeneous formation, Applied Catalysis B: Environmental, 168–169 (2015) 183-194

[23] S. Rtimi, Indoor light enhanced photocatalytic ultra-thin films on flexible non-heat resistant substrates reducing bacterial infection risks, MDPI-Catalysts 7 (2017) 57.

[24] A. Fujishima, X. Zhang, D. Tryk, TiO_2 photocatalysis and related surface phenomena, Surf. Sci. Repts. 63 (2008) 515-582.

[25] A.A. Assadi, A. Bouzaza, D. Wolbert, Photocatalytic oxidation of Trimethylamine and Isovaleraldehyde in an annular reactor: Influence of the Mass Transfer and the relative humidity. Journal of Photochemistry and Photobiology A: Chemistry 236 (2012) 61-69.

[26] A. A. Assadi, J. Palau, A. Bouzaza, J. Penya-Roja, V. Martinez-Soria, D. Wolbert, Abatement of 3-methylbutanal and trimethylamine with combined plasma and photocatalysis in a continuous planar reactor, Journal of Photochemistry and Photobiology A: Chemistry 282 (2014) 1-8.

[27] M. Pachoalino, J. Kiwi and W. Jardim,Gas phase photocatalytic decontamination using polymer supported TiO_2. Appl. Cat. B, 68 (2006) 68-73.

[28] M. I. Mejía, J. M. Marín, G. Restrepo, L. A. Rio, C. Pulgarín, J. Kiwi, Preparation, testing and performance of TiO_2/Polyester for the degradation of gaseous methanol, Appl. Catal. B. 2010, 94 166-172.

[29] D. Farhanian, F. Haghighat, Photocatalytic oxidation air cleaner: Identification and quantification of by-products, Building and Environment, 72 (2014) 34-43.